The trend towards a warmer and wetter climate observed in arid and semi-arid areas of northwest China from 1959 to 2019

Environmental Research Communications

PAPER

The trend towards a warmer and wetter climate observed in arid and semi-arid areas of northwest China from 1959 to 2019

Shijun Zheng[1,2], **Bing Zhang**[1,2], **Dailiang Peng**[1,*], **Le Yu**[3], **Binbin Lin**[4], **Yuhao Pan**[1,2] and **Qiaoyun Xie**[5,*]

[1] Key Laboratory of Digital Earth Science, Aerospace Information Research Institute, Chinese Academy of Sciences, Beijing 100094, People's Republic of China
[2] University of Chinese Academy of Sciences, Beijing 100049, People's Republic of China
[3] Ministry of Education Key Laboratory for Earth System Modeling, Department of Earth System Science, Tsinghua University, Beijing 100084, People's Republic of China
[4] Texas A&M University, College Station, TX 77843 United States of America
[5] University of Technology Sydney, Faculty of Science, Sydney NSW 2007, Australia
[*] Authors to whom any correspondence should be addressed.

E-mail: pengdl@aircas.ac.cn **and** Qiaoyun.Xie@uts.edu.au

Keywords: warm–wet trend, northwest China, drought

OPEN ACCESS

RECEIVED
4 August 2021

REVISED
9 November 2021

ACCEPTED FOR PUBLICATION
15 November 2021

PUBLISHED
26 November 2021

Abstract

The observed trend towards a warmer and wetter climate in northwest China is a controversial issue lacking sufficient scientific research. Based on monthly meteorological data from 201 weather stations in northwest China and surrounding regions from 1959 to 2019, we calculated potential evapotranspiration using Penman-Monteith (PM) equation. By analyzing the spatial–temporal variations in temperature and precipitation and by studying changing drought trends, we systematically explored the climate trends in northwest China over the past 60 years. Our findings include: (1) From 1959 to 2019, during the growing season, there was a significant upward trend in temperature across northwest China. The most obvious trend, ranged between 0.4 °C–0.6 °C per decade, was observed in northern Qinghai and northeastern Xinjiang. On a per-month basis, the average temperature increased in all months, with April showing a maximum rate of 0.41 °C per decade. (2) The amount of precipitation in the growing season increased in most regions, especially in western Xinjiang and Qinghai. The areas of reduced precipitation were mainly concentrated in the south of Gansu and Ningxia, the west of Shaanxi and the northeast of Xinjiang. The average precipitation also increased in all months, with June showing a maximum change rate of 1.8 mm per decade. (3) There were obvious spatial differences in the climate trends in northwest China with the warming shifting from areas of bare land to grassland and the trend towards increased rainfall shifting from grassland to bare land. These effects were most obvious in Xinjiang's Tarim Basin. (4) From 1959 to 2019, the degree of drought in northwest China significantly decreased in most areas. The areas where drought decreased and precipitation increased were fairly consistent, which produced a strong spatial correlation between them.

1. Introduction

The sixth IPCC assessment report stated that the global average surface temperature had increased by 0.85 °C from 1880 to 2012 and that global warming would continue in the future (IPCC 2021). Climate warming has caused damage to our living environment (Jeppesen *et al* 2020, Chen 2021). Due to its profound impact, climate warming has become an enormous challenge for scientists and government agencies (Meehl *et al* 2005, Tian *et al* 2011). Northwest China, which is one of the driest regions in the world at its latitude, contains 85% of the country's arid and semi-arid areas (Chen *et al* 2012). Most of this region has a temperate continental climate with the eastern part also being affected by the East Asian monsoon. The climate of the region thus has the characteristics of low precipitation, high precipitation variability and a high frequency of drought. The special

geo-climatic conditions result in high environmental vulnerability and high sensitivity to climate change. Given the high amounts of solar radiation, the agricultural productivity of northwest China is high. Therefore, it is of practical and far-reaching strategic significance to investigate the trend towards a warmer and wetter climate in northwest China, not only from an academic perspective, but also because of its importance to the environmental, socio-economic and other systems in this region.

A large number of researchers have studied temperature and precipitation in northwest China in recent decades and some scholars have found that both the frequency and intensity of precipitation in the region has increased significantly (Zhai *et al* 2005, Wang *et al* 2013, Guo *et al* 2020). The rate of precipitation increase found during 1960 to 2010 was about 0.61 mm per year (Li *et al* 2016). However, this rate of increase varied greatly according to the type of landscape—rates of 10.15 mm, 6.29 mm and 0.87 mm per decade were found for the mountain, oasis and desert areas respectively (Li *et al* 2013). In addition to the changes in precipitation, the air temperature has also increased at a rate of 0.3 °C–0.4 °C per decade (Chen *et al* 2010). The rate of temperature increase also varied according to the type of landscape, with rates of 0.325 °C, 0.339 °C and 0.360 °C per decade being found for mountain, oasis and desert areas respectively (Li *et al* 2013). These studies have demonstrated that both temperature and precipitation have increased drastically in northwest China in recent decades. However, there is a lack of combined analysis of the temperature and precipitation to comprehensively and systematically investigate the trend towards a warmer and wetter climate in Northwest China.

It was not until the early 21st century that some research on the trend towards a warmer and wetter climate in northwest China was conducted. For example, Shi *et al* (2002) reported a gradual increase in precipitation in the northwest of the Yellow River basin since 1987 and that the climate of northwest China was changing from 'warm and dry' to 'warm and wet' (Shi *et al* 2002). Shi *et al* (2007) also pointed out that the trend towards a warmer and wetter climate was multifaceted: as well as an increase in temperature and precipitation, it also included, for example, glacier melting, an increase in runoff, a raising of the water levels of inland lakes, an increase in the frequency of floods, an improvement in vegetation and a reduction in sandstorms (Shi *et al* 2007). Since then, studies based on different methods have indicated that there is a clear trend towards a warmer and wetter climate in northwest China. Some researchers constructed a dryness index to analyze the increase in rainfall by directly using precipitation and evaporation data from meteorological stations (Wang *et al* 2007). The results clarified that, for the northwest region as a whole, as well as for the westerly climate zone and the plateau climate zone, there has been a significant trend towards a wetter climate and there was an abrupt change from dry to wet conditions in the mid-1970s. However, in the dry, southeastern part of northwest China, which has a monsoon climate, there was an abrupt change from wet to dry in the early 1990s. Some researchers have used meteorological station data to calculate the potential evaporation in northwest China and then constructed a dryness index by combining this with precipitation data. These researchers found that there has been an obvious increase in the dryness index in northwest China, indicating a trend towards a wetter climate (Liu *et al* 2013, Zhang *et al* 2021). In addition, other researchers have analyzed the land water availability (LWA), which reflects the amount of land water resources, against the background of climate change and found that both precipitation and evaporation have increased during the warm season in northwest China. The increase in precipitation was found to be greater than the increase in evaporation, suggesting an increase in the LW, and a trend towards wetter conditions in northwest China (Wang *et al* 2020).

However, after constructing a dryness index to study climate trends in northwest China, some researchers came to the opposite conclusion that the region was becoming drier (Yang *et al* 2012). In addition, some research analyzing the standardized precipitation evapotranspiration index (SPEI) showed that northwest China has been becoming progressively drier over the past 50 years (Ren *et al* 2014).

Previous studies show that there is still a debate as to whether northwest China has become warmer and wetter in recent decades; in some cases contradictory conclusions have even been drawn based on the same index. The reasons for this may be that most of these studies were limited to meteorological station data or were carried out a low spatial resolution and thus were not able to accurately detect changes in temperature and precipitation over a large area. In particular, the meteorological stations located in northwest China are sparsely and unevenly distributed and cannot record and describe the meteorological situation across the whole region. In addition, most previous studies were conducted before 2010, and cannot be used to analyze more recent overall climate trends in northwest China.

In this study, we calculated the potential evapotranspiration using data from 201 meteorological stations in northwest China and the surrounding areas from 1959 to 2019. Combined with altitude, longitude and latitude data, we then obtained spatial temperature, precipitation and potential evapotranspiration maps (with a resolution of 0.083 degrees) by interpolation. We then used these maps to produce systematic spatio-temporal results of the trend towards a warmer and wetter climate in northwest China.

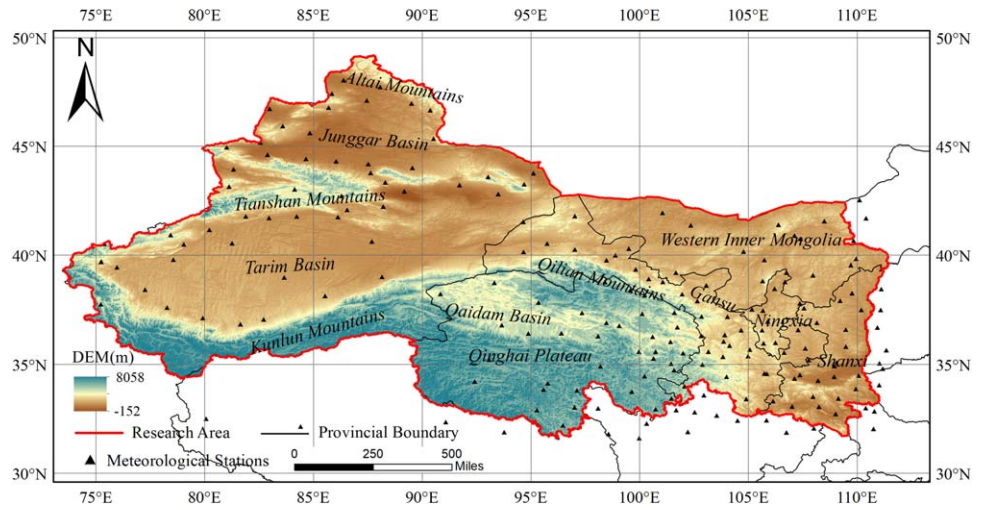

Figure 1. Location of the study area—northwest China.

2. Methodology

2.1. Study area

The study area used for this research consisted of northwest China, including Shaanxi Province, Gansu Province, Qinghai Province, Ningxia Hui Autonomous Region, Xinjiang Uygur Autonomous Region and western Inner Mongolia (figure 1). This region is located in the interior of Eurasia and to the north and northeast of the Qinghai–Tibet Plateau, China; it occupies about 30% of the total area of China. Most of the region lies at an altitude of over 3000 m, with the highest altitude being 8058 m and the lowest –152 m. The geomorphology of the region is complicated: many mountain ranges and basins are contained within the region. The Altai Mountains are located in the north of the region, the Tianshan Mountains in the west, the Kunlun Mountains and Qinghai Plateau in the south, and the Qilian Mountains in the middle. The Junggar Basin, Tarim Basin, and Qaidam Basin are located between these high mountains. The complex terrain means that warm, wet air from the ocean is unable to travel a long way inland and penetrate the mountain barriers. The result is that the region experiences drought conditions and large diurnal temperature ranges.

2.2. Data and methods

2.2.1. Calculation of potential evapotranspiration

Potential evapotranspiration refers to the maximum possible evaporation of the wet land surface under certain meteorological conditions. To calculate it, we collected monthly average meteorological data from 1959–2019 at 201 stations in northwest China from the National Meteorological Information Center (figure 1) and used the Penman-Monteith (PM) equation (Allen *et al* 1998) as shown in formula (1). These meteorological data include maximum temperature, minimum temperature, average temperature, relative humidity, wind speed at 2 m above ground surface, atmospheric pressure and sunshine hours.

$$ET_0 = \frac{0.408\Delta(R_n - G) + \gamma\dfrac{900}{T+273}\mu_2(e_s - e_a)}{\Delta + \gamma(1 + 0.34u_2)} \tag{1}$$

Where ET_0 represents potential evapotranspiration (in mm day^{-1}), R_n represents net radiation (MJ m^{-2} day^{-1}), G represents soil heat flux (MJ m^{-2} day^{-1}). T represents average temperature (°C), μ_2 represents wind speed at 2 m above ground surface (m s^{-1}), e_s represents saturation vapor pressure at air temperature (kPa), e_a represents actual air vapor pressure (kPa), Δ represents slope of saturation vapor pressure/temperature curve (kPa °C^{-1}), and γ represents psychrometric constant (kPa °C^{-1}). R_n was calculated as

$$R_n = 0.77 \times \left(0.2 + 0.79\left(\frac{n}{N}\right)\right)R_{so} - \sigma\left(\frac{T_{\max,k}^4 + T_{\min,k}^4}{2}\right)(0.56 - 0.25\sqrt{e_a})\left(0.1 + 0.9\left(\frac{n}{N}\right)\right) \tag{2}$$

in which $T_{\max,k}$ and $T_{\min,k}$ are maximum and minimum temperature, respectively; n and N are sunshine hours and possible maximum sunshine hours, respectively; R_{so} represents shortwave radiation and given by

$$R_{SO} = [0.75 + 2(\text{Altitude})/100000]R_a \tag{3}$$

in which R_a represents solar radiation at the top of the atmosphere. The quantities e_s, e_a, Δ and γ are computed according to

$$e_S = 0.6108 \exp\left[\frac{17.27T}{T + 237.3}\right] \tag{4}$$

$$e_a = e_s RH_{\text{mean}} \tag{5}$$

$$\Delta = \frac{4098e_s}{(T + 237.3)^2} \tag{6}$$

$$\gamma = 0.000665P \tag{7}$$

in which T is average temperature; RH_{mean} is relative humidity; P is atmospheric pressure.

2.2.2. Spatial rasterization of meteorological station data

Multiple regression and residual interpolation was applied to the meteorological data to perform spatial rasterization based on 1-km DEM data. This gridding strategy has been shown more accurate than direct interpolation methods (Liao *et al* 2003). Multiple regression is a statistical interpolation method. The basic idea was to decompose a meteorological element into two parts: a regular component and an irregular component. The regular components included the longitude, latitude, altitude and other quantifiable elements; the irregular components consisted of the residuals between the regression simulation of the meteorological elements and the regular components (Liao and Li 2003). The procedure consisted of the following steps. (1) A regression equation linking the dependent variables (the meteorological data) and the independent variables (the longitude, latitude and altitude of the meteorological stations) was constructed. Next the regular elements—the gridded meteorological data—were obtained by putting the gridded independent variables into the equation that had been established. (2) The residuals between the observation and the estimated data at the meteorological stations were interpolated to acquire the gridded residuals, which constituted the irregular component of the meteorological element. (3) The spatial rasterization of the meteorological station data was obtained by adding the regular and irregular components. The multiple regression equation that was used was

$$W = a \cdot X + b \cdot Y + c \cdot Z + R \tag{8}$$

where, W is the meteorological element (in this study, the air temperature, precipitation and potential evapotranspiration); X is the longitude, Y is the latitude, Z is the elevation and R is the residual; a, b and c are the coefficients of the regression equation.

2.2.3. Climate tendency rate

The climate tendency rate reflects the changing trends in regional climatic elements and is expressed by a linear regression equation (Qian *et al* 2010):

$$X = a + bT \tag{9}$$

Here X represents the climate element with sample size n $(x_1, x_2, x_3, \ldots, x_n)$; T represents a time-series of length n $(t, t_2, t_3, \ldots, t_n)$; a is a constant and b is the regression coefficient. a and b can be calculated using the least-squares formula:

$$a = \bar{x} - b\bar{t} \tag{10}$$

$$b = \frac{\sum_{i=1}^{n} x_i t_i - \frac{1}{n}\left(\sum_{i=1}^{n} x_i\right)\left(\sum_{i=1}^{n} t_i\right)}{\sum_{i=1}^{n} t_i^2 - \frac{1}{n}\left(\sum_{i=1}^{n} t_i\right)^2} \tag{11}$$

$\bar{x}$ and $\bar{t}$ are estimated as follows:

$$\bar{x} = \frac{1}{n}\sum_{i=1}^{n} x_i, \quad \bar{t} = \frac{1}{n}\sum_{i=1}^{n} t_i \tag{12}$$

The square of the correlation coefficient (R^2) between X and T is expressed as

$$R^2 = \sqrt{\frac{\sum_{i=1}^{n} t_i^2 - \frac{1}{n}\left(\sum_{i=1}^{n} t_i\right)^2}{\sum_{i=1}^{n} x_i^2 - \frac{1}{n}\left(\sum_{i=1}^{n} x_i\right)^2}} \tag{13}$$

2.2.4. Combining Sen's slope and the Mann–Kendall test

Compared with linear regression, the use of Sen's slope, which is associated with the Mann–Kendall test, is less affected by data error and minimizes the impact of outliers, thus improving the estimation accuracy. This method is one of the most effective for analyzing trends in long sequences of data (Burn and Elnur 2002). The formula for calculating the Mann–Kendall statistic (S) can be represented as follows (Mohd Wani *et al* 2017):

$$S = \sum_{i=1}^{n-1} \sum_{j=i+1}^{n} sgn(x_j - x_i) \tag{14}$$

$$sgn(\theta) = \begin{cases} +1 \ \theta > 0 \\ 0 \ \theta = 0 \\ -1 \ \theta < 0 \end{cases} \tag{15}$$

where $i = 1, 2, 3, \ldots$ *to* $n - 1$ and $j = i + 1, \ i + 2, \ i + 3, \ldots$ *to* n; x_i and x_j are the values for years i and j, respectively. The standard normal statistic, Z, is given by

$$Z = \begin{cases} \dfrac{S - 1}{\sqrt{var(S)}} \ S > 0 \\ 0 \ 0 \\ \dfrac{S + 1}{\sqrt{var(S)}} \ S < 0 \end{cases} \tag{16}$$

$$Var(S) = \sqrt{\frac{t(t - 1)(2t + 5)}{18}} \tag{17}$$

where t is the number of years. The estimates of Sen's slope can be given as

$$\beta = Median\left(\frac{x_j - x_i}{j - i}\right) 1 < i < j < n \tag{18}$$

When $\beta > 0$, there is an upward trend in the values in the sequence; when $\beta < 0$, the trend is downward. In addition, when $Z > 1.65$ ($Z > 1.96$, $Z > 2.58$), it means that this trend passes the significance test at the 0.1 (0.05, 0.01) level.

2.2.5. Dryness index

Precipitation and evapotranspiration are the two most important elements in the surface water balance and need to be included for an objective understanding of a trend towards increasing wetness (Wang *et al* 2020). In this study, we calculated the dryness index using both precipitation and potential evapotranspiration data. We then analyzed the trends in this index in order to produce a comprehensive description of the trend towards increasing wetness in northwest China. The dryness index was defined as (Zhang *et al* 2016):

$$I_{AI} = \frac{E_{TO} - P_{RE}}{E_{TO}} \tag{19}$$

This index is applicable to northwest China; the larger the value of the dryness index, the more serious the drought. E_{TO} is the potential evapotranspiration. P_{RE} is the precipitation.

2.2.6. Isoline trend surfaces

The isoline trend surfaces, by means of which the inter-annual variations in temperature and precipitation were analyzed in this study, were obtained by processing the annual isolines corresponding to a certain value of the temperature or precipitation. Isoline trend surfaces can reflect inter-annual spatial variations because their pixel values represent years. The process used to generate isoline trend surfaces was as follows:

(1) The annual isolines corresponding to specific values of temperature or precipitation for the period 1959–2019 were constructed.

(2) The isolines from step (1) were collected and the spatial range of the trend surfaces determined. As far as possible, the trend surfaces were designed to include all of the isolines but a few outliers were excluded.

(3) Images corresponding to the spatial range of the trend surfaces determined in step (2) were generated. Each pixel value in these images was obtained by interpolation between the isolines within a certain distance.

2.2.7. Isolate the anthropogenic and natural forcing components

To attribute the trends of climatic warming and wetness to anthropogenic forcing (such as increased greenhouse gases or manmade aerosol) and natural forcing (such as volcanic eruptions), the historical all-forcing datasets

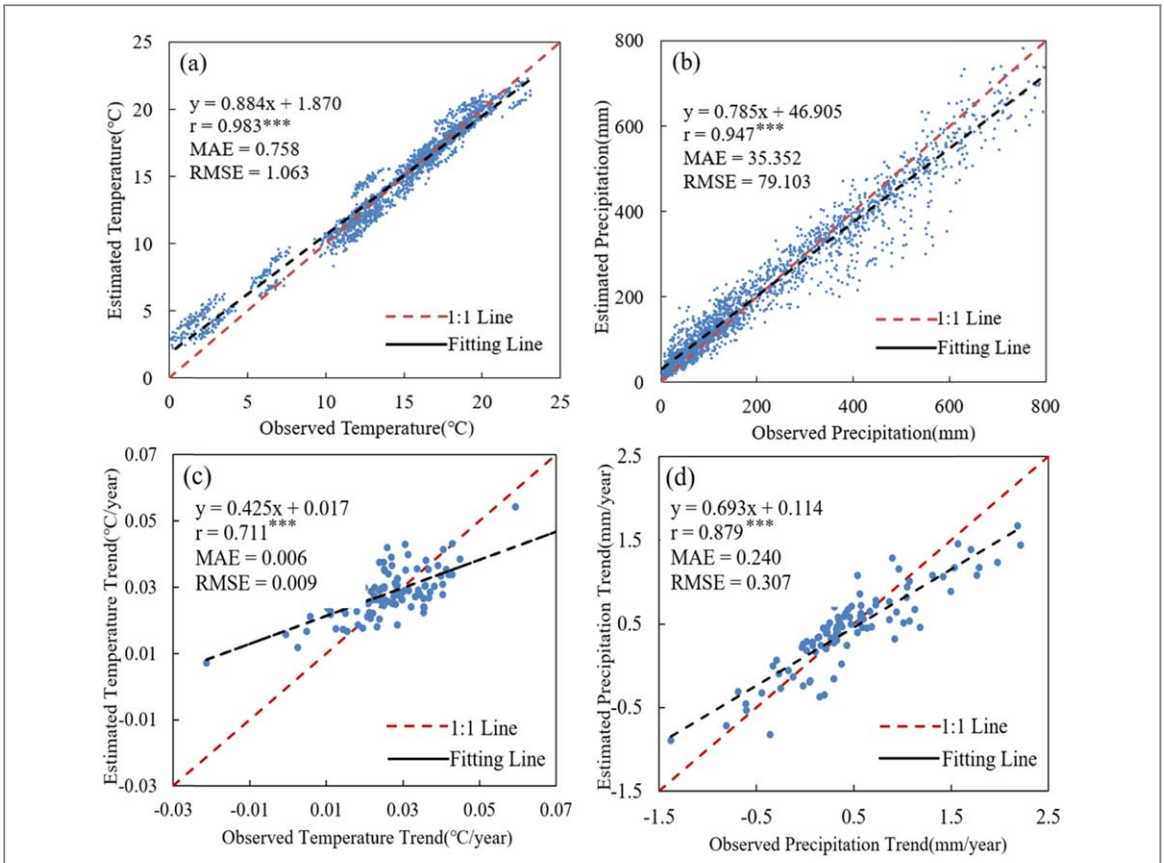

Figure 2. Validation tests for the spatial rasterization results of (a) temperature and (b) precipitation, and the trends of (c) temperature and (d) precipitation from 1959 to 2019.

were obtained from CMIP6 (Dong and Dai 2017, IPCC 2021). We take the temperature for example in equations (20), (21) to calculate its anthropogenic or natural forcing components. Specifically, the annual time series of temperature was regressed onto natural forcing(Smith *et al* 2021) over the period from 1959 to 2019, and then the regressed part was subtracted from the original temperature to get the anthropogenic forcing component.

$$T\_Forcing = a + b \times Forcing \tag{20}$$

$$T\_new = T\_original - T\_Forcing \tag{21}$$

where $T\_Forcing$ is the regressed part of the temperature, which is associated with natural forcing, a and b are the regression coefficients using data from 1959–2019. $T\_original$ is the original temperature, and T_new is the residual without the natural forcing. We attributed the remaining trends in T_new to temperature variations under anthropogenic forcing (Zhao *et al* 2018). The anthropogenic and natural forcing precipitation are calculated by equations (20), (21).

3. Results and discussion

3.1. Spatial distribution of temperature and precipitation

Figures 2(a) and (b) present the comparisons between observed and estimated values of temperature and precipitation, using 80% of the meteorological data for the spatial rasterization and the rest for validation. The results of r (the correlation coefficient), MAE (the mean absolute error) and RMSE (root mean square error) were 0.983, 0.758, and 1.063, respectively for temperature, and were 0.947, 35.352 and 79.103 respectively for precipitation ($p < 0.01$). Figures 2(c) and (d) present the comparisons between the trend of observed and estimated values of and precipitation. The r, MAE and RMSE values for temperature trend were 0.711, 0.006, and 0.009 respectively, and were 0.879, 0.240, and 0.307, respectively for precipitation trend ($p < 0.01$).

Figure 3 shows the spatial distribution of temperature and precipitation in the growing seasons in northwest China from 1959 to 2019. During this period, the average temperature in different parts of the region ranged between 0 °C and 30 °C. There were obvious spatial differences with low temperatures occurring in the south of the region and high temperatures occurring in the north and east. Due to the differences in altitude, the average

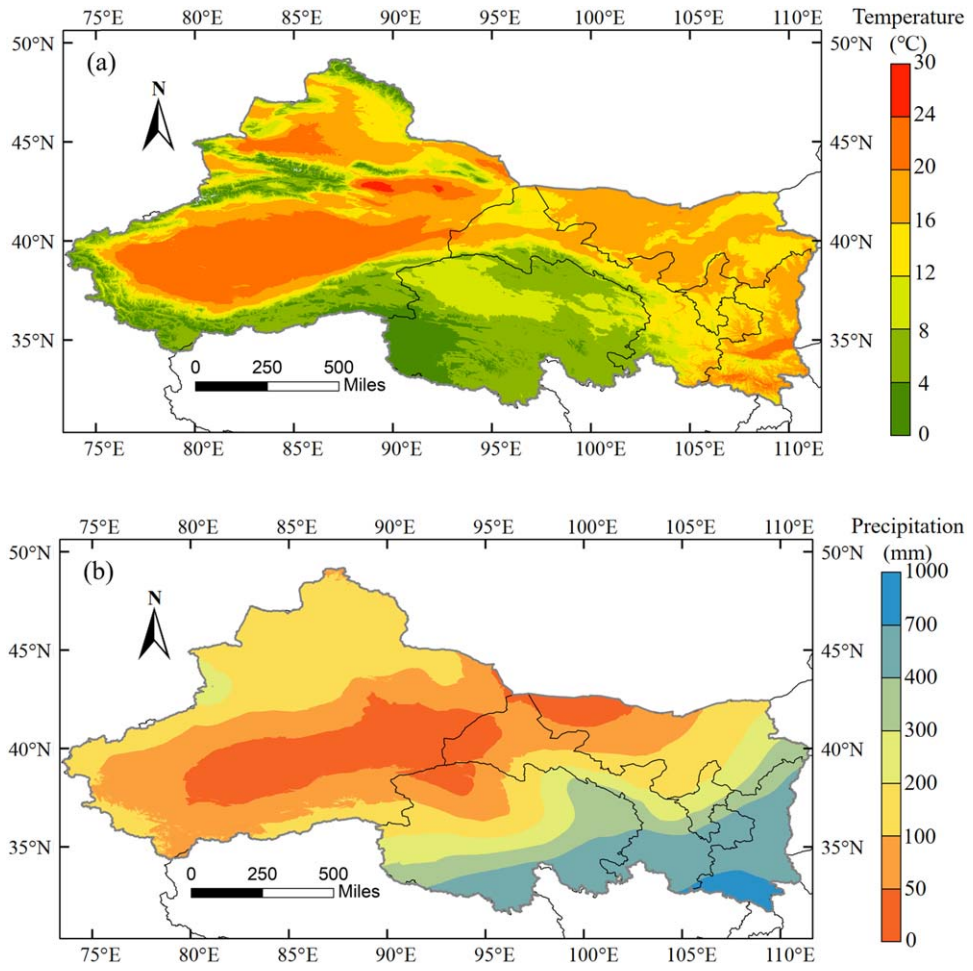

Figure 3. Spatial distribution of (a) temperature and (b) precipitation during the growing season in northwest China.

temperature in the Qinghai Plateau, Qilian Mountains, Kunlun Mountains, Tianshan Mountains and Altai Mountains was generally below 8 °C, whereas the temperature in the Tarim Basin and the Junggar Basin was generally higher. In particular, the temperature in most parts of the Tarim Basin—the hottest part of northwest China—was above 20 °C. During this period, the average precipitation in most parts of northwest China was around 200 mm. The precipitation gradually increased from the central areas (desert) to the southeast and northwest. Xinjiang showed the lowest precipitation in northwest China, within which, the highest precipitation was in the north and the lowest precipitation was in the centre and south. The low precipitation was particularly obvious in the Tarim Basin, generally below 100 mm. In Qinghai, Gansu and the west of Inner Mongolia, the precipitation showed an obvious increasing trend from northwest to southeast and is less than 50 mm in northwest and more than 300 mm in southeast. Precipitation amounts in Ningxia and Shaanxi were generally over 100 mm and 300 mm, respectively with an increasing pattern from north to south. In particular, Shaanxi showed the most abundant precipitation in northwest China, i.e. above 400 mm in most areas and 700–1000 mm in the south.

3.2. Inter-annual variations in temperature and precipitation during the growing season

Figure 4 shows the inter-annual variations in temperature and precipitation during the growing season in northwest China. From 1959 to 2019, the overall temperature trend was upwards at a rate of 0.31 °C per decade ($p < 0.01$). We divided the study period into six phases of ten years and analyzed the temperature change within each period. The rates of change for 1959–1969, 1969–1979, 1979–1989, 1989–1999, 1999–2009 and 2009–2019 were –0.37, 0.23, 0.24, 1.09, 0.30 and 0.07 °C per decade, respectively. The temperature in the study area decreased during 1959–1969 and then showed an increasing trend in each decade from 1969 to 2019. The slope increased and reached the maximum during the period 1989–1999, followed up by lower rate of changes from 1999 to 2019. From 1959 to 2019, the amount of precipitation in northwest increased at a rate of 4.81 mm per decade ($p < 0.01$). The rates of change in precipitation during the 1959–1969, 1969–1979, 1979–1989, 1989–1999, 1999–2009 and 2009–2019 decades were all positive: 6.31, 3.52, 10.32, 7.22, 5.72 and 31.96 mm per

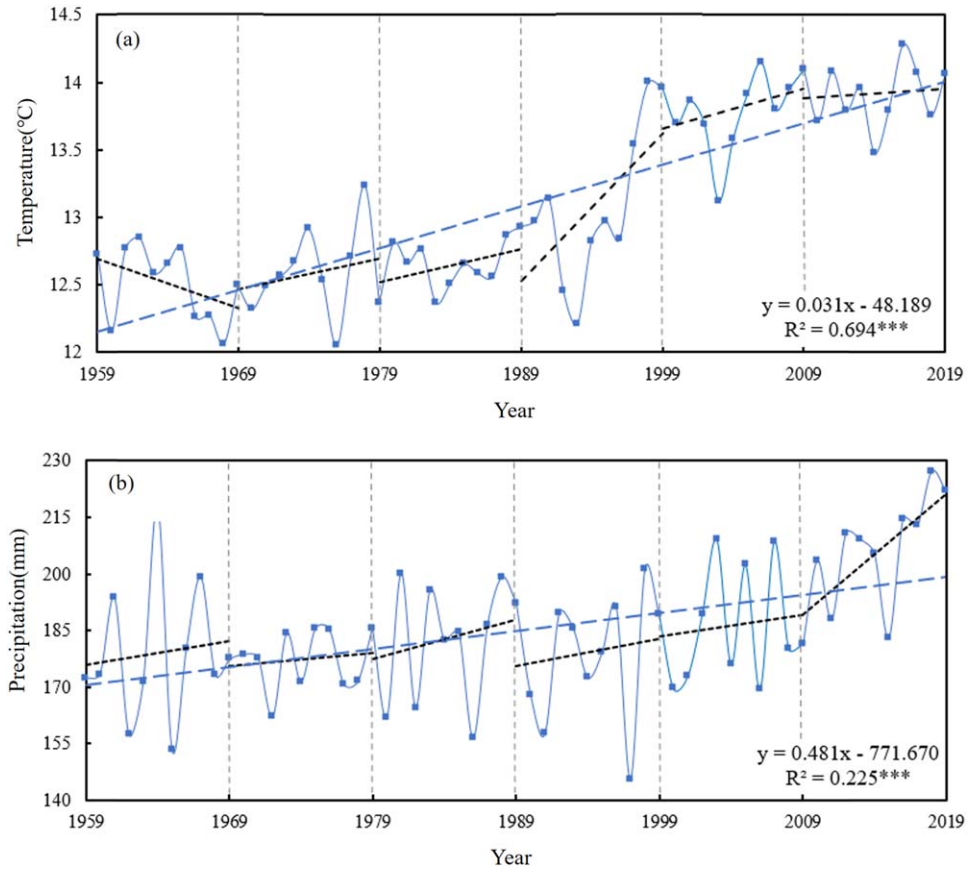

Figure 4. Overall and ten-year variations in (a) temperature and (b) precipitation in northwest China from 1959 to 2019.

decade, respectively. The lowest slope was from 1969 to 1979 and the highest was from 2009 to 2019. These results pass the significance test at the 0.05 level.

Figure 5 shows the maps of temperature and precipitation trends in northwest China during 1959–2019. There was a significant increase in temperature across the study area ($p < 0.05$). The trend was below 0.3 °C per decade in the Tarim Basin and the surrounding areas, parts of Junggar Basin and the southeast corner of Qinghai Province. More severe warming trend, 0.4 °C–0.6 °C per decade, occurred in northern Qinghai and northeastern Xinjiang. In terms of precipitation, there was an increase in 87.53% of the total study area especially in western Xinjiang and Qinghai, where, in most areas, the increase passes the significance test at the 0.05 level. The rate of increase in precipitation exceeded 5 mm per decade in most parts of western Xinjiang and 10 mm per decade in most parts of Qinghai. Areas with reduced precipitation were mainly in the south of Gansu and Ningxia, the west of Shaanxi and the northeast of Xinjiang, but these decreasing trends were not significant except for a small part of northeast Xinjiang. The rate of precipitation change was relatively low and not significant, between 0–3 mm per decade, in most parts of eastern Xinjiang and the north of Gansu. The eastern part of the study area did not show any significant trends of precipitation change.

3.3. Inter-annual variations in monthly temperature and precipitation

The per month (April to October) trends in average temperature from 1959 to 2019 in our study area are shown in figure 6(a) and variations of temperature per-decade are shown in figure 6(b). Each month (from April to October) showed a significant warming trend ($p < 0.01$) across 60 years, at the rate of 0.41 °C, 0.23 °C, 0.32 °C, 0.35 °C, 0.27 °C, 0.30 °C, and 0.28 °C per decade, respectively. The inter-decade variations in monthly average temperature (figure 6(b)) revealed that temperature decreased in most months during 1959–1969, and increased in every month during 1989–1999. A decrease in the average April temperature during the period 1959–1989, followed by a dramatic increase over the next 30 years, especially during the period 1989–1999 (0.212 °C per decade). The average July temperature showed a marked increase from 1979 to 1999 but fell during the other decades. The temperature in September fell significantly from 1959 to 1969 but has been increasing since then. In October, the temperature decreased from 1959 to 1969 and in the most recent decade, but increased in the other periods.

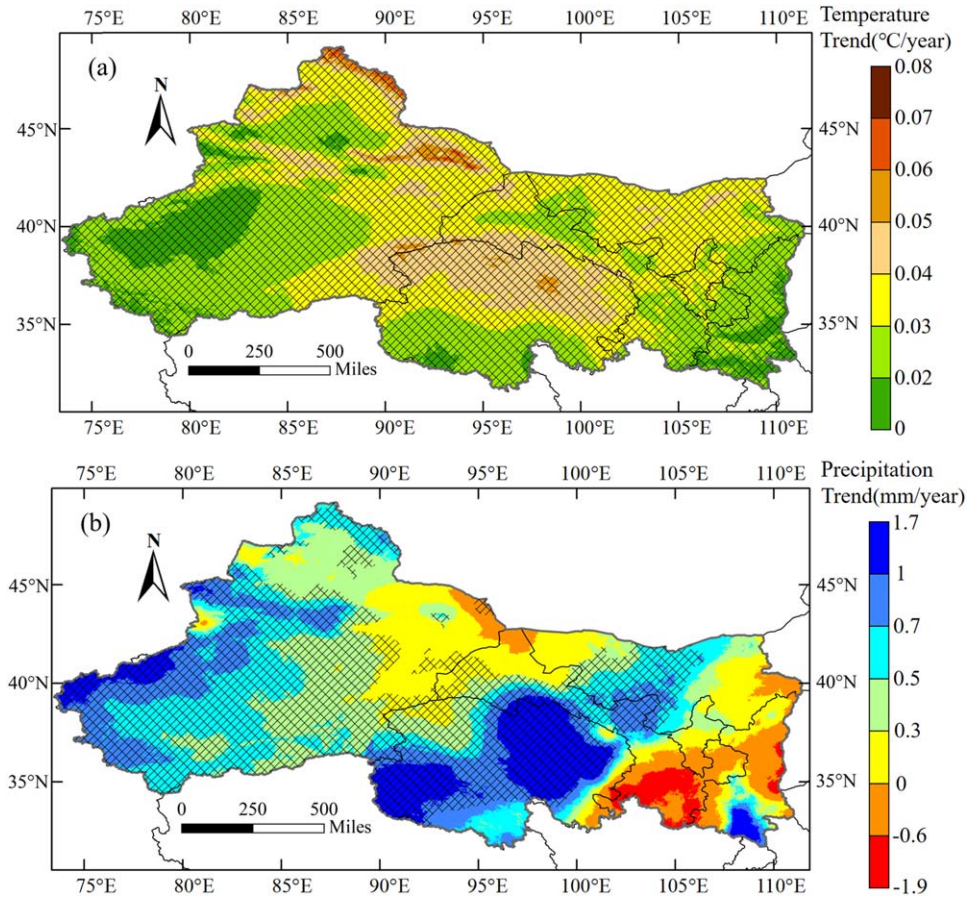

Figure 5. Maps of trend from 1959 to 2019: (a) temperature and (b) precipitation. Regions that pass the significance test at 0.05 level ($p < 0.05$) were marked by crosshatch.

Figure 7 shows maps of temperature trends during 1959–2019 per month (April to October). A warming trend per month occurred across the study area except for southern Shaanxi in June and August and a few parts of southern Xinjiang in August, with differences in the rate of change among different months and the most dramatic warming occurred in April, confirming the results in figure 6. In April, the rate of significant warming in most areas exceeded 0.3 °C per decade ($p < 0.05$), with some northern areas exceeding 0.5 °C per decade. In May, the rate of warming was below 0.3 °C per decade in most regions of the study area and below 0.2 °C per decade in most parts of Xinjiang. The spatial patterns of rates of warming in June were similar to those in July, with the higher rates occurring in the centre of the study region (mainly found in the east of Xinjiang, the north of Qinghai and the west of Inner Mongolia) and lower rates in the east and west (western part of Xinjiang, in Shaanxi and in Ningxia). August exhibited similar patterns of warming to October, i.e. high rate of warming occurred in the north of Xinjiang and northern Qinghai whilst the lower rate of warming occurred in western Xinjiang, Shaanxi, and Ningxia. Overall, the rate of warming in northern Qinghai was relatively high in all months, and it was generally lower in Ningxia, Shaanxi and western Xinjiang.

Similar to the temperature analysis, the per month (April to October) trend of average precipitation from 1959 to 2019 in our study area are shown in figure 8(a) and variations of precipitation per-decade are shown in figure 8(b). For each month from April to October, the precipitation increased at the rate of 0.30 mm, 0.87 mm, 1.80 mm, 0.59 mm, 0.51 mm, 0.54 mm, and 0.12 mm per decade, respectively. The highest and lowest rates of increase occurred in June ($p < 0.05$) and October, respectively. In terms of per-decade variations in precipitation, in June, the precipitation decreased dramatically from 1989–2009 but increased during other periods, especially in 1979–1989 and 2009–2019. In July, an increase occurred in 1969–1979 and 1989–2009 and a decrease occurred in the other decades. August showed an increased precipitation in 1989–2019, particularly in 2009–2019. In September, there was an increase during the periods 1959–1979 and 1999–2009 but a decrease during the other periods. Generally, within each decade of the study period, the number of months with a precipitation increase was greater than the number with a precipitation decrease. Also, in the most recent decade showed a significant increase in precipitation in most months.

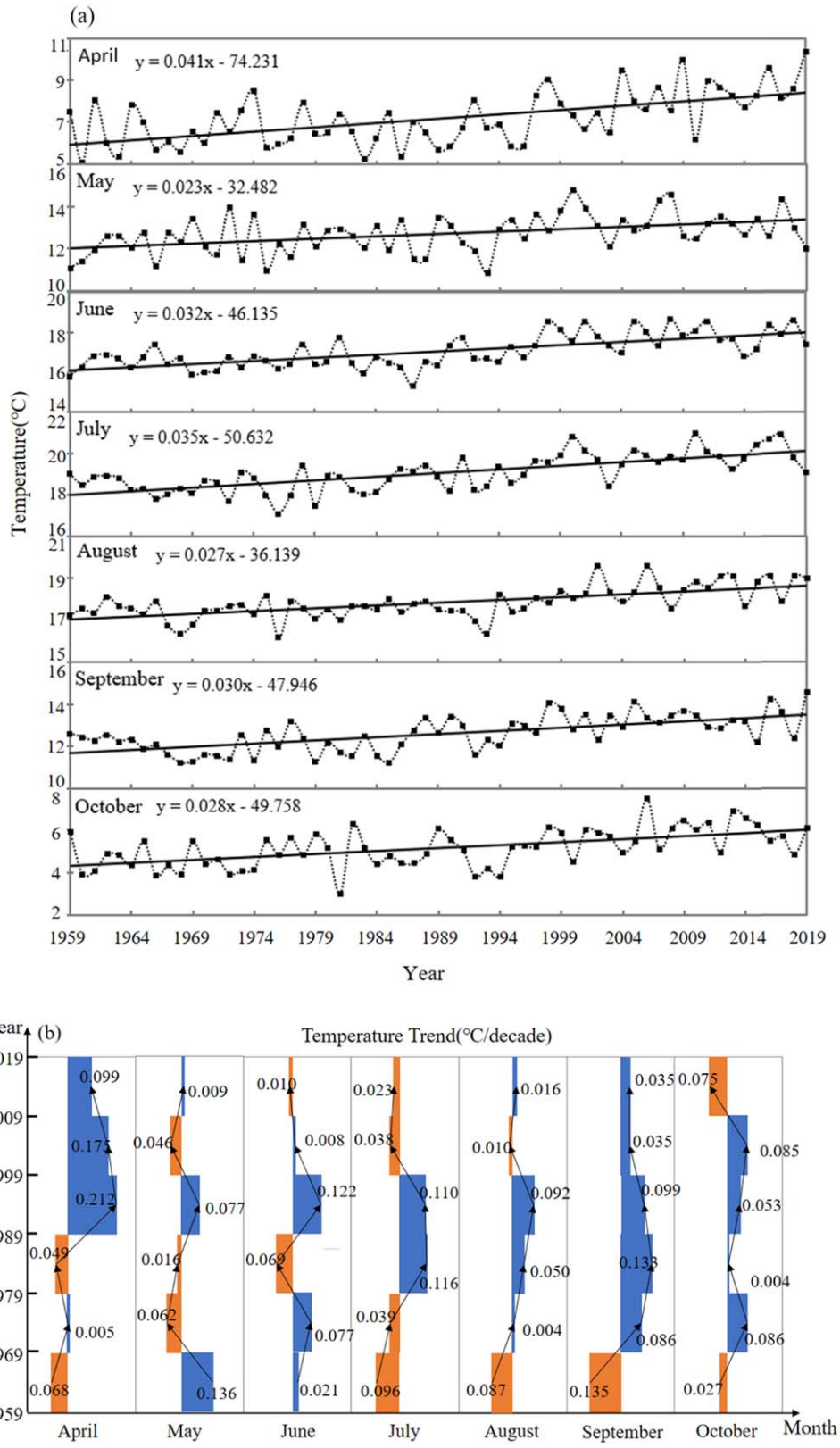

Figure 6. (a) Overall trends in monthly temperature during the growing season (April–October). (b) Ten-year changes in temperature for each month during the growing season.

Figure 9 presents maps of precipitation trends per month (April to October) during 1959–2019 in the study area. The trend varied from month to month. In April, the precipitation showed little change (–0.1 to 0.1 mm per decade) in most parts of central and southern Xinjiang and northern Qinghai, significantly increased in northern Xinjiang and southern Qinghai ($p < 0.05$), and decreased in Ningxia and Shaanxi, and particularly in southern Shaanxi ($p < 0.05$). In both May and June, the precipitation increased in most regions of the study

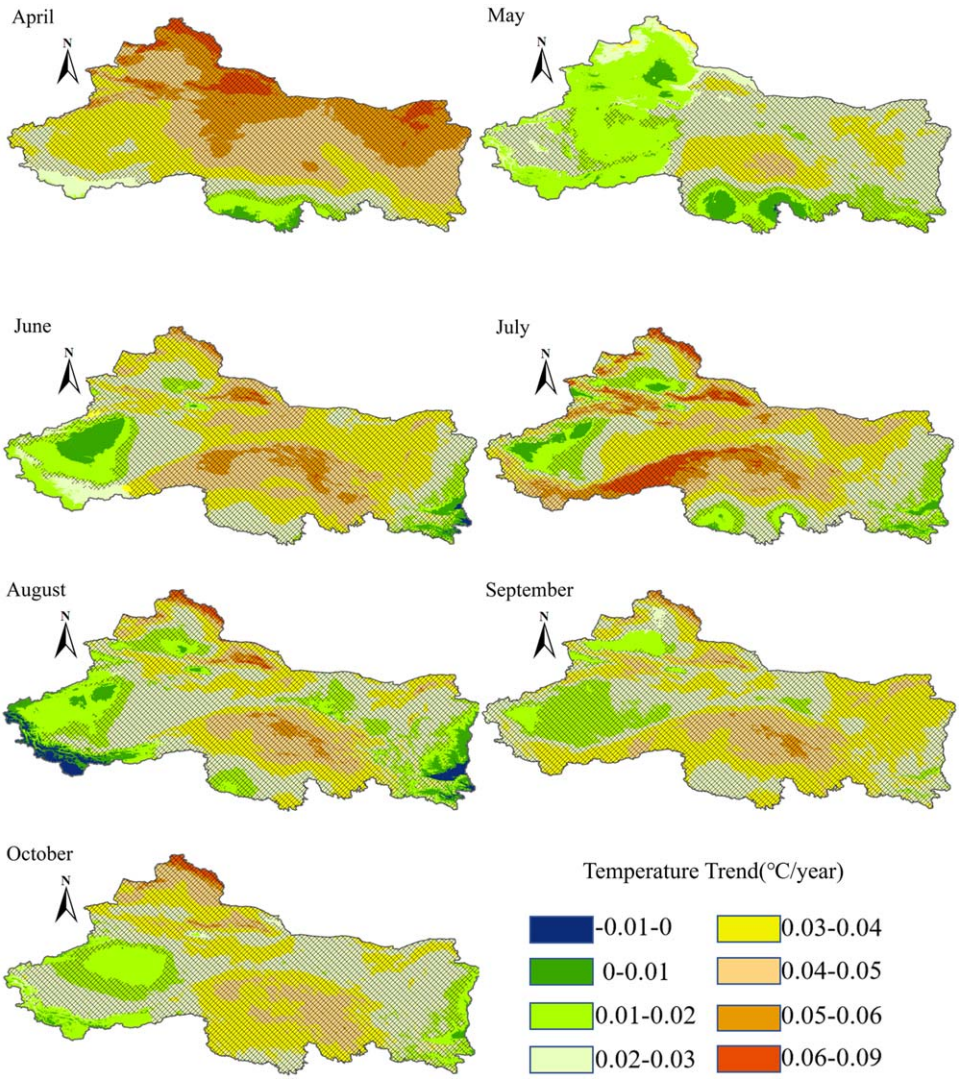

Figure 7. Maps of temperature trends during 1959–2019 per month (April to October). Regions that pass the significance test at 0.05 level were marked by crosshatch.

area, especially in the southern part of Qinghai in May (>2 mm per decade) and in western Xinjiang, central Qinghai and the eastern part of the study area in general in June ($p < 0.05$). In July, there was an increase in precipitation in northern Qinghai and western Xinjiang and a decrease in northeastern Xinjiang, southern Qinghai, southern Gansu and southern Ningxia. In August, the precipitation in the south of Xinjiang and the north of Qinghai increased markedly, however, the eastern part of the study area showed a decreasing trend. In September, the precipitation increased in central and southern Qinghai and western Inner Mongolia and decreased in the southeast of the study area. The precipitation trend for October is similar to that for April: the amount of precipitation in central and southern Xinjiang, northern Qinghai and western Inner Mongolia is almost unchanged, and areas with an increase are mainly concentrated in northern Xinjiang and southern Qinghai. To sum up, the precipitation showed the predominant increase in Qinghai and a decrease in the eastern part of the study area.

3.4. Spatial patterns of the inter-annual variations in temperature and precipitation

To investigate the spatial patterns of the inter-annual variations in temperature and precipitation from 1959 to 2019, we calculated the trend surfaces for the 50 mm, 100 mm, 150 mm and 200 mm precipitation isolines and the 10 °C, 15 °C and 20 °C temperature isolines, as shown in figures 10 and 11.

Figure 10 shows that the positions of the 10 °C, 15 °C and 20 °C temperature isolines moved from bare lands to areas of grasslands during 1959 to 2019. Given that temperature is greatly affected by elevation, and as there are many mountains and basins in the study area, the temperature isolines followed the intersections between different types of terrain, i.e. the 10 °C isoline mainly located in the north of Qinghai Province, the 15 °C isoline generally followed the margin of the Junggar Basin in northern Xinjiang, and the 20 °C isoline mainly located in

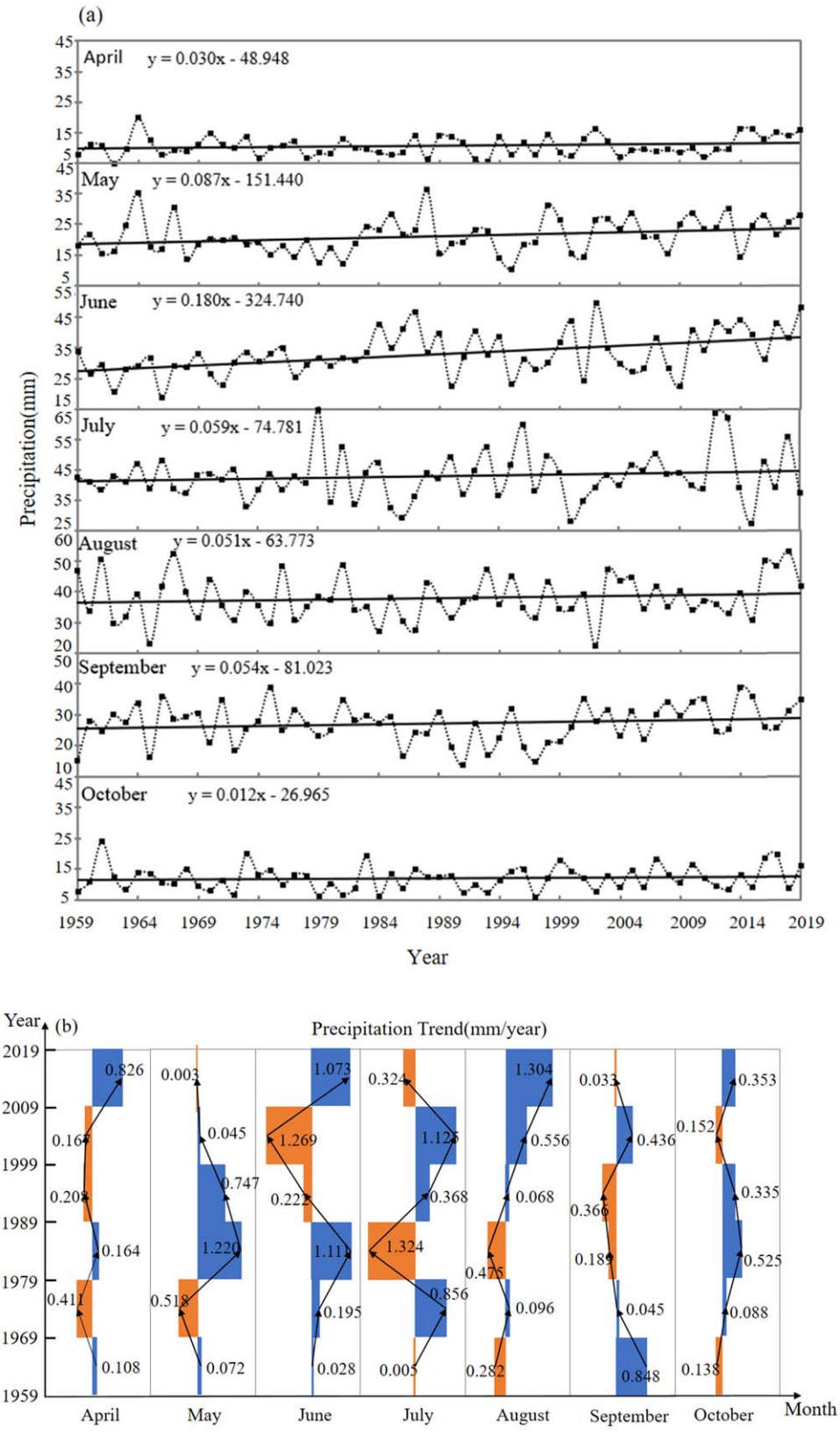

Figure 8. (a) Overall trends in monthly precipitation during the growing season (April–October). (b) Ten-year changes in precipitation for individual months during the growing season.

the south of the Junggar Basin and the edge of the Tarim Basin. In Xinjiang, the 15 °C isoline moved from bare lands in the Junggar basin to the surrounding grasslands, and the 20 °C isoline moved from the bare lands in the Tarim Basin to the surrounding grasslands. In Qinghai Province, the 10 °C isoline moved from the bare lands in the Qaidam Basin to the surrounding grasslands.

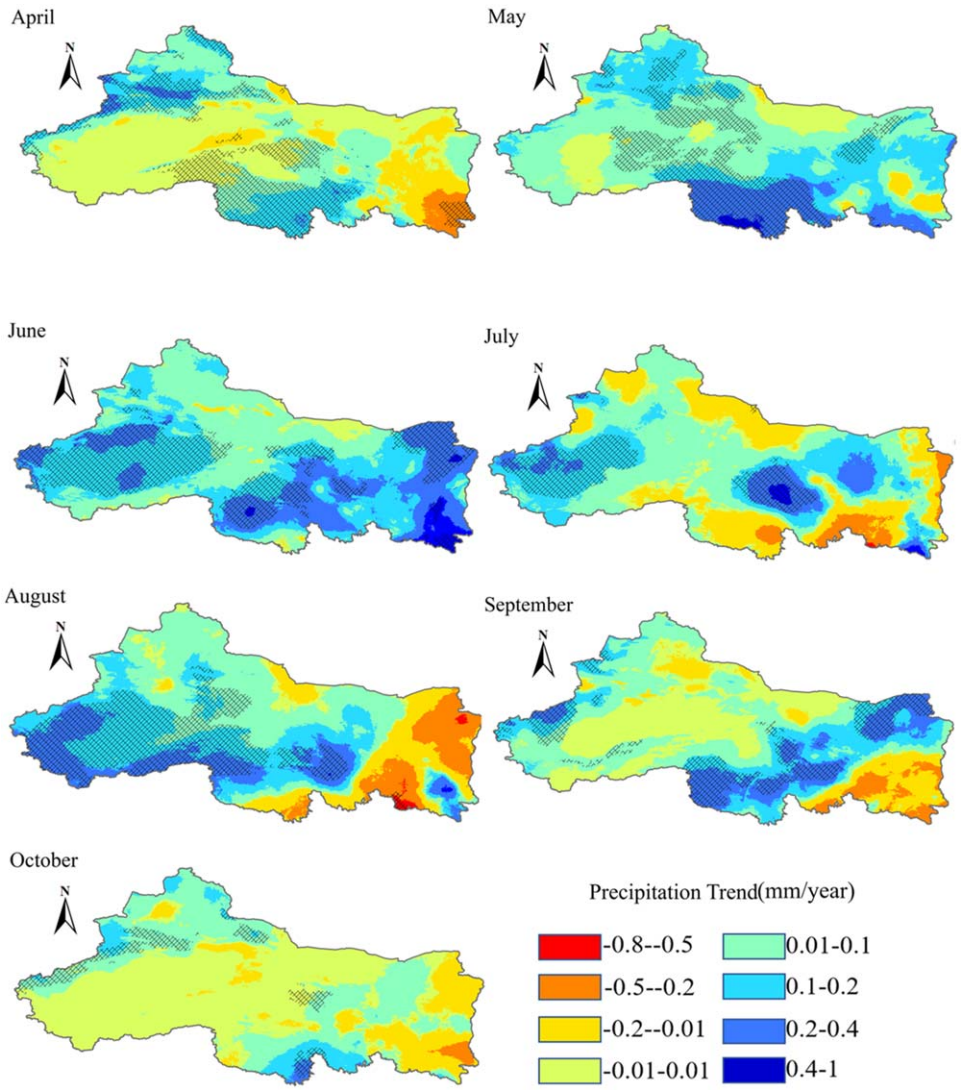

Figure 9. Maps of precipitation trends during 1959–2019 per month (April to October). Regions that pass the significance test at 0.05 level were marked by crosshatch.

Figure 11 shows that there were obvious changes in the 50 mm, 100 mm, 150 mm and 200 mm isolines during 1959 to 2019. Generally, these isolines moved from grasslands to bare lands. In Xinjiang, the 50 mm surface was rather fragmented and moved from the outside to the inside of bare lands in central Xinjiang. The 100 mm and 150 mm surfaces also showed clear movements from farmlands and grasslands in western Xinjiang to bare lands in central Xinjiang. In Qinghai and northern Gansu, all of the four precipitation isolines moved from grasslands to bare lands. Most parts of western Inner Mongolia covered by bare land showed no clear shifts of the precipitation isolines.

We found the temperature and precipitation isolines moved in opposite directions during 1959 to 2019. Most areas at higher altitude in the study area were covered by grasslands, with low temperature and abundant precipitation. In contrast, areas at lower elevations were mostly bare lands, with high temperature and low precipitation. As both temperature and precipitation increased, the temperature and precipitation isolines moved in opposite directions.

3.5. Inter-annual variations in the dryness index

Figure 12 shows the inter-annual variations of the dryness index during the growing season in the study area, which showed a significant downward trend during the 60-year study period, indicating a mitigation of drought. The rates of dryness index changes during 1959–1969, 1969–1979, 1979–1989, 1989–1999, 1999–2009 and 2009–2019 were –0.009, –0.005, –0.014, –0.006, 0, and –0.038 per decade, respectively. All decades showed a decreasing trend of the dryness index, except 1999–2009 during which no trend was observed. Similar to precipitation trends, the change in the dryness index was at its highest rate in the most recent decade ($p < 0.05$).

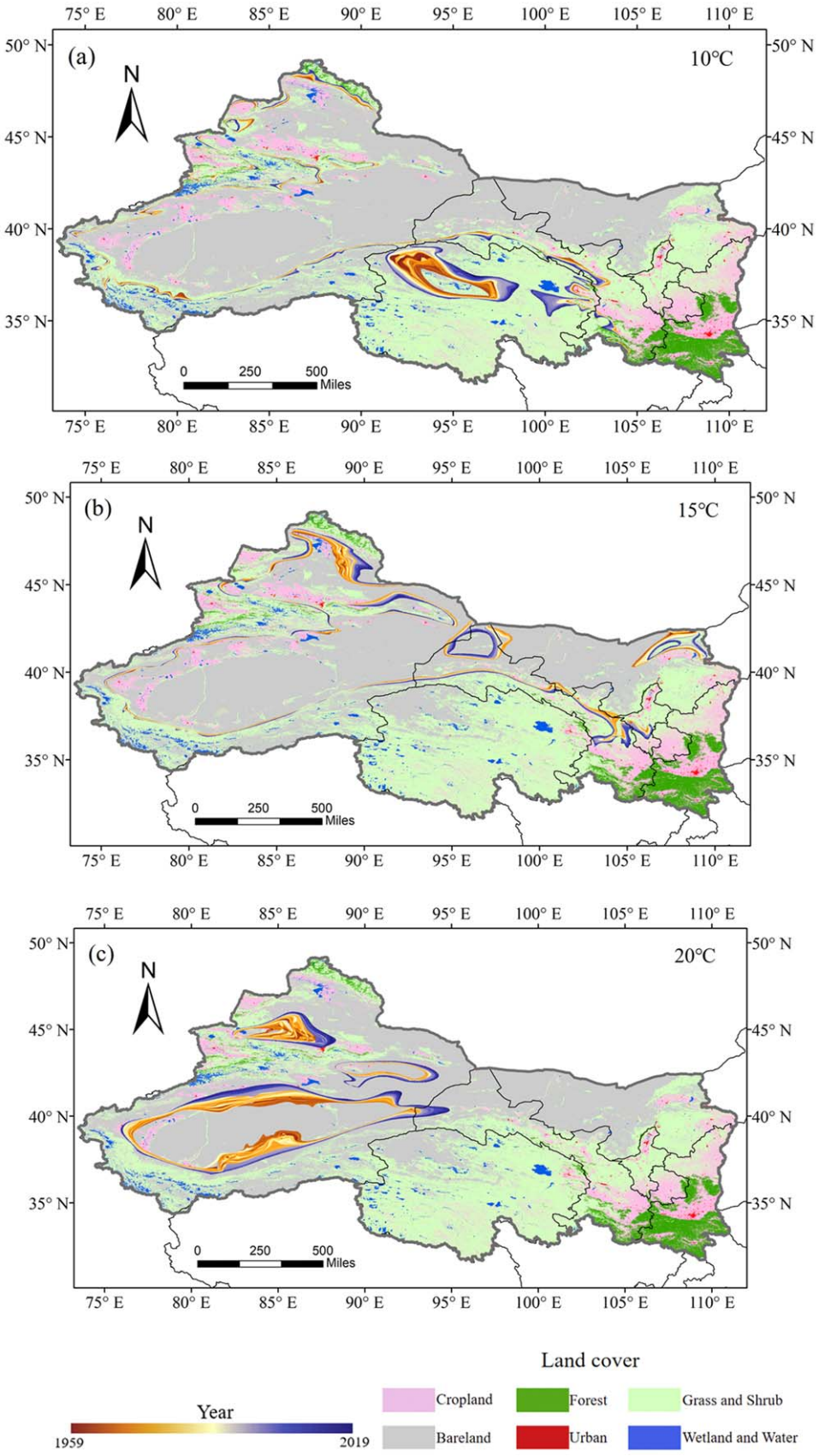

Figure 10. Movement of temperature isoline surfaces in northwest China during the period 1959–2019. (a)–(c) represent the 10 °C, 15 °C and 20 °C surfaces, respectively.

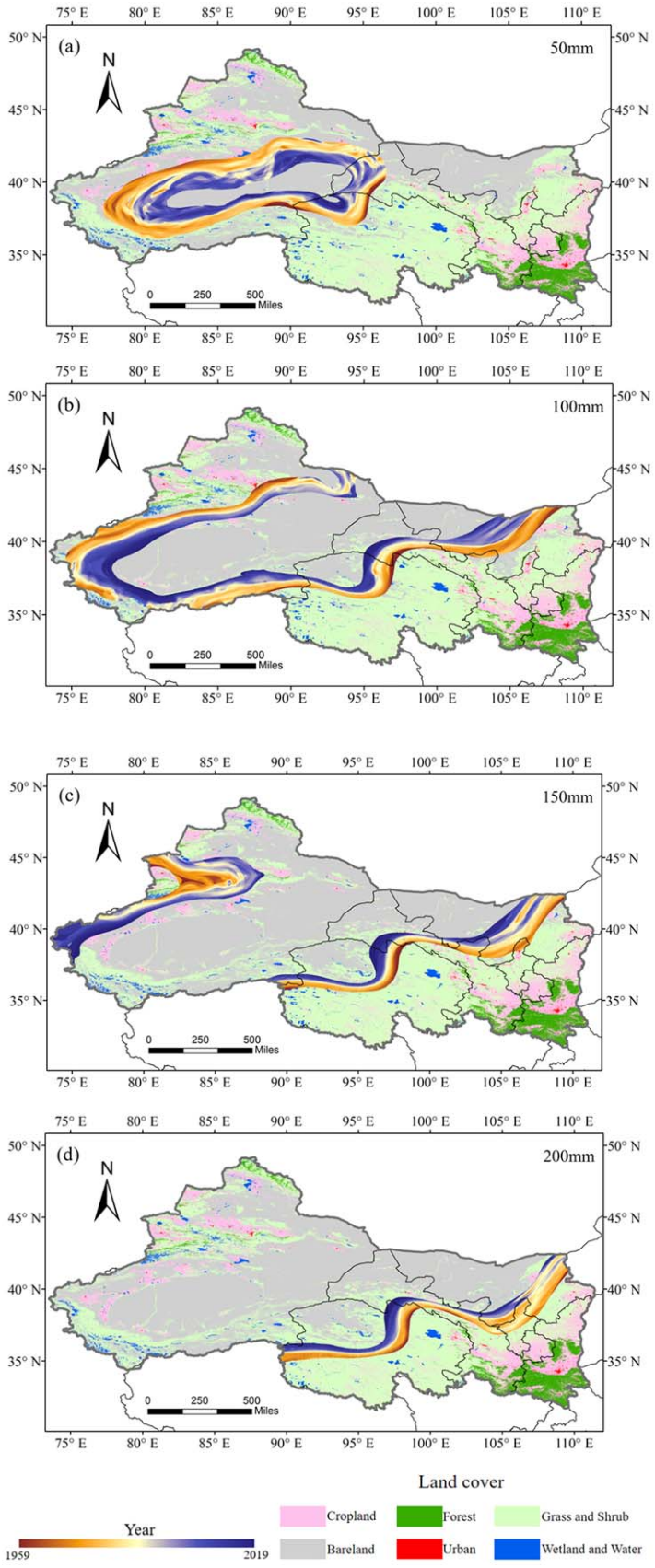

Figure 11. Movement of precipitation isoline surfaces during the period 1959–2019 in northwest China. (a)–(d) present the 50 mm, 100 mm, 150 mm and 200 mm surfaces, respectively.

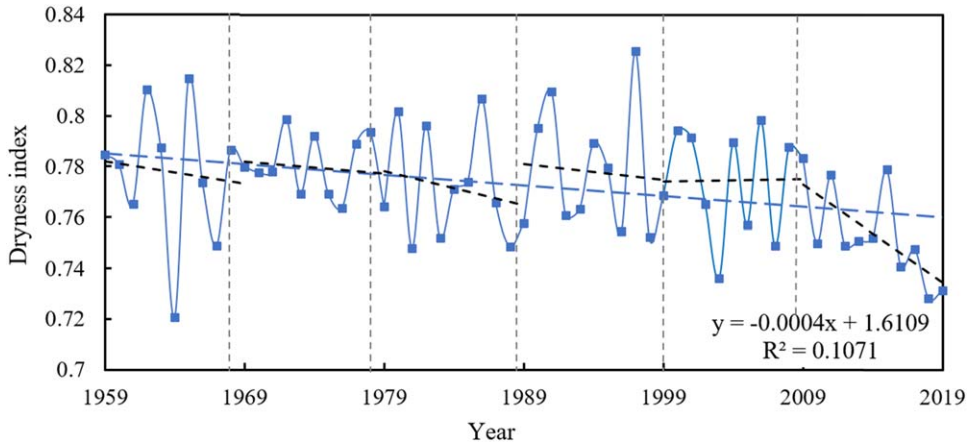

Figure 12. Overall and per-decade variations in the dryness index in our study area from 1959 to 2019.

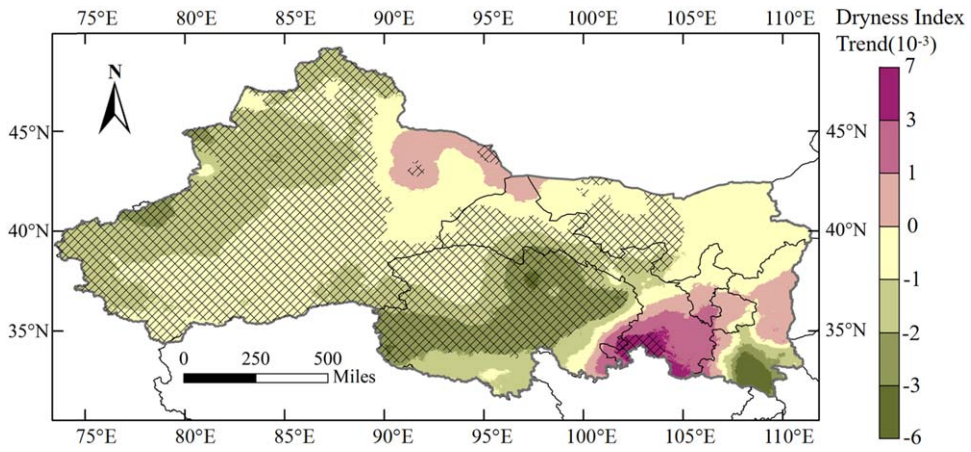

Figure 13. Spatial trend distributions from 1959 to 2019 of the dryness index with regions that pass the significance test at 0.05 level marked by crosshatch.

The spatial trend distributions of dryness index map, as shown in figure 13, exhibits a significant decrease in most regions, especially in western Xinjiang and Qinghai ($p < 0.05$) and an increase in the south of Shaanxi, Ningxia and Gansu, and the northeast of Xinjiang. These results, together with the spatial details of the inter-annual variation in precipitation (figure 5), show that the regions with reduced drought were consistent with the regions with increased precipitation. As such, the spatio-temporal changes in precipitation and the drought index in the study area over the past 60 years have been consistent, suggesting that precipitation has a significant influence on drought and plays an important role in the trend towards a wetter climate.

3.6. Analysis of the trend towards a warmer and wetter climate in northwest China from 1959 to 2019

In this study, we analyzed the spatial–temporal variations in temperature and precipitation in northwest China from 1959 to 2019 as well as the drought index. We combined these results with potential evapotranspiration data to analyze the changing drought trends and to study the trend towards a warmer and wetter trend in northwest China at multiple spatial–temporal scales.

During growing season, the entire study area exhibited a warming trend from 1959 to 2019, with the average temperature of the area increased by 0.31 °C per decade. These results are consistent with a previous study that temperature in arid northwest China increased by 0.35 °C per decade during 1961 to 2006 (Chen *et al* 2010). Note that warming trend did not occur across all regions in the earlier study. For example, the local trend in the Kuqa area of Xinjiang was decreasing. More recent research has shown that there was an overall warming in arid northwest China from 1961 to 2018 (Zhang *et al* 2021), which is consistent with the results of our study. The discrepancies between these research findings may be caused by the differences in observation period. The timespan covered by prior research was too short to reveal the pattern of temperature changes that has occurred in recent decades. In terms of precipitation, we found that 87.53% of the study area became wetter

(4.8 mm per decade) from 1959 to 2019. Previous studies reported that precipitation increased in 93.4% of the arid northwest China between 1961 and 2018 (Zhang *et al* 2021), and Li *et al* (2016) reported that the precipitation in northwest China from 1960 to 2010 increased by 6.1 mm per decade. The differences in spatial patterns and rate of changes between previous studies and our study could be the result of different study areas: previous studies focused on smaller areas and did not include Gansu, southern Ningxia and Shaanxi. To test this hypothesis, we reduced the size of the research area to the same as in those studies and found similar results: the precipitation increased in 92% of the area from 1961 to 2018 and precipitation in northwest China from 1960 to 2010 increased by 5.9 mm per decade.

According to our per decade analysis of the results, the trends of temperature and precipitation during different decades between 1959 and 2019 were quite different, suggesting that the climate trends of the entire period are not representative of each decade. For example, from 1959 to 1969, northwest China became colder, in line with other study (Chen *et al* 2010). Between 1969 and 2019, northwest China showed continuous warming, with the rate of warming increased and then declined and the maximum warming rate occurred between 1989 and 1999, agreeing with Shi *et al* (2007) that the temperature rose sharply from the 1980s to the 1990s. From 1959 to 2019, overall, the northwest of China became much wetter and the most obvious increase occurred in the most recent decade (31.96 mm per decade), which agrees with the findings of Zhang *et al* (2021).

The trends towards warmer and wetter conditions in northwest China have not been simultaneous. The most significant warming occurred during the 1990s, whereas the trend towards wetter conditions was most obvious in the most recent decade (as shown in figure 4). Spatially, the most obvious warming occurred in northern Qinghai and northeastern Xinjiang, whereas the trend towards increased precipitation has been most obvious in western Xinjiang as well as in the eastern and western parts of Qinghai (as shown in figure 5).

The temperature and precipitation trends were also analyzed per month, because the sowing and main growth periods of many crops were calculated by month (Sacks *et al* 2010, Kara *et al* 2012, Yan *et al* 2020) and greatly affected by temperature and precipitation conditions (Frasier *et al* 1987, Chauhan *et al* 2014). Therefore, an analysis of the conditions in different months is of great significance to the crop harvest. However, per-month trends were understudied in previous studies, which mainly focused on analysis at the annual and seasonal scales. This study concentrated on the change in conditions from 1959 to 2019 for individual months and the results indicate that, for all months, there has been a trend towards warmer and wetter conditions in northwest China. The warming has been most obvious in April and the least evident in May; the increase in precipitation has been most evident in June and least obvious in October (as shown in figures 6 and 8). However, it is not the case that, for every month, the conditions became progressively warmer and wetter from 1959 to 2019. From 1959 to 1969, most months became colder, whereas from 1989 to 1999 there was warming in all months. In the most recent ten-year period, there was a clear increase in precipitation in most months (as shown in figures 6 and 8).

Studies based on time-series data can reveal the inter-annual variations in an overall trend towards warmer and wetter conditions and have become the most widely used method in the study of these trends in northwest China. Moreover, this study also looked at the spatial variations and analyzed how these variations have changed. It can be seen from the displacement of the isolines of temperature and precipitation that occurred during the study period, as the temperature isolines moved from regions of bare land towards the grassland but the precipitation isolines moved in the opposite direction (figures 10 and 11). These trends were most obvious in the Tarim Basin in Xinjiang, which consists mostly of bare land with relatively high temperatures and low precipitation surrounded by grassland with lower temperatures and higher precipitation. The precipitation isolines moved from outside the bare lands to the inside while the temperature isolines shifted from inside the bare lands to the surrounding grasslands. Considering that the growth of vegetation depends on both temperature and precipitation, the question of whether this displacement will make the grassland spread into the bare land or make the original grassland more luxuriant is worth further study.

The raw temperature and precipitation data that are available for the study of climate trends in northwest China are limited, so we combined precipitation and potential evapotranspiration to construct a drought index. The analysis of the drought index shows that the degree of drought in most parts of northwest China has decreased in the past 60 years and that, for the region as a whole, this decrease has been significant. These results are consistent with the existing research (Zhang *et al* 2021). In addition, for northwest China, the dryness index dropped significantly between 1960 and 2010 (Liu *et al* 2013): this is also in line with the annual change in the dryness index illustrated in figure 10 in this study. We also found a strong spatial correlation between drought and precipitation in northwest China. The regions with reduced drought are almost identical to areas with increased precipitation (see figures 5 and 13).

Global warming induced by greenhouse effect has caused the warmer trend in northwest China(Bao *et al* 2004). The increasing vegetation greenness in northwest China reduces surface reflectance and increases absorption of solar short-wave radiation, which may also cause warming in this area (Bonan *et al* 1992, Piao *et al* 2005). Previous studies have found that the increasing evaporation from the Indian Ocean due to global

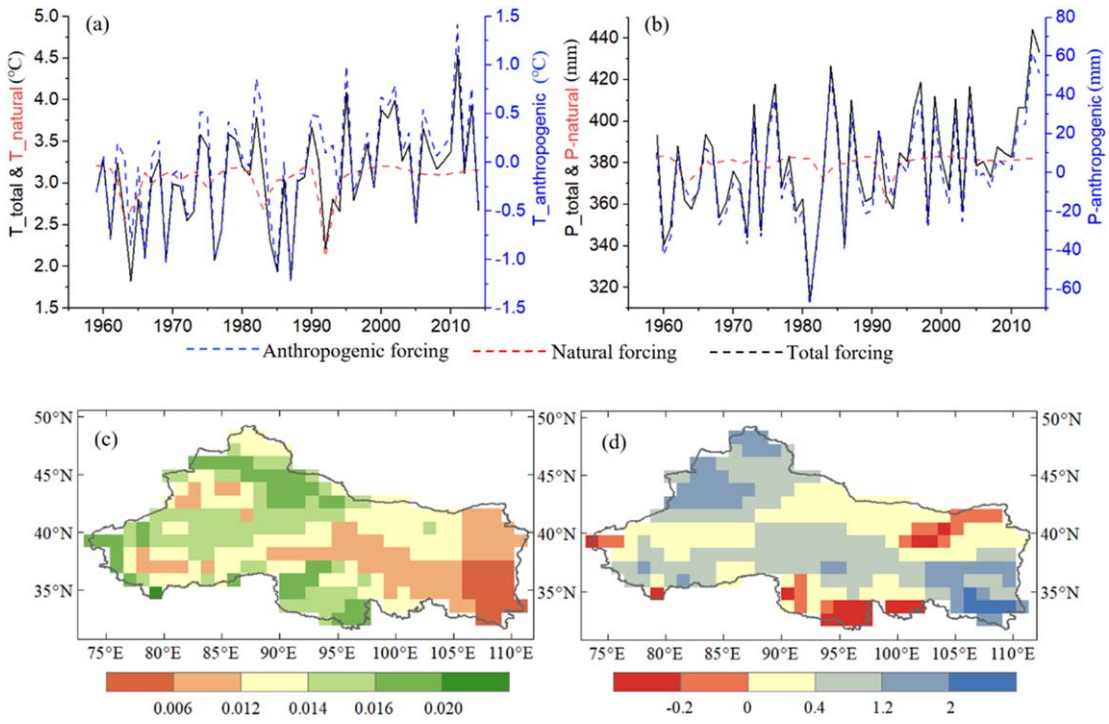

Figure 14. The trends of (a) natural forcing temperature (T_natural) and total temperature (T_total) (left axis), anthropogenic forcing temperature (T_anthropogenic) (right axis); (b) natural forcing precipitation (P_natural) and total precipitation (P_total) (left axis), anthropogenic forcing precipitation (P_anthropogenic) (right axis). The (c) anthropogenic forcing temperature trends and (d) anthropogenic forcing precipitation trends at the pixel level.

warming brought more water vapor to northwest China, and the gradually glacier runoff in the high mountains, enhancing westerly flow, monsoon also increased atmospheric water vapor content in northwest China (Lu *et al* 2005, Piao *et al* 2010).

Our trend attribution analysis (based on equations (20), (21)) shows that the anthropogenic forcing made the largest contribution to both trends of temperature and precipitation from 1959–2019, while the contribution from the natural forcing was much smaller (figures 14(a), (b)). The contribution of anthropogenic forcing is 85.58% to the trend of temperature and 93.16% to the trend of precipitation. Therefore, the anthropogenic forcing is the main contributor to the trend of warming and wetness in northwest China. It was found that the anthropogenic forcing induces strong warming trends in the western and southern region, and induces strong wetness trends in the northwestern, central and southeastern region (figures 14(c), (d)).

Based on the results of this study and the comparison with previous studies, we found that: (1) from the temporal perspective, we observed a trend towards a warmer and wetter climate in northwest China over the past 60 years; and (2) from spatial perspective, the warming trend moved from bare lands to areas of grasslands, while the trend towards increased precipitation shifted toward the opposite direction.

4. Conclusions

From 1959 to 2019, there was an overall increase in the temperature and precipitation during the growing seasons in northwest China. The rates of increase were 0.31 °C per decade and 4.81 mm per decade, respectively, meaning that northwest China is generally becoming warmer and wetter. During the growing season from 1959 to 2019, while northwest China as a whole had a significant increase in temperature and the precipitation increased in 87.53% of northwest China. By dividing the study period into six ten-years periods, we found that the temperature decreased during 1959–1969 but increased during the following decades. The rate of temperature changes first increased and then decreased, reaching a maximum between 1989 and 1999. The precipitation significantly increased throughout the study period, with the most obvious increase occurring during the period 2000–2019.

There were obvious differences between the trends for different months. The rates of temperature change for all months were positive for the period from 1959 to 2019, with the maximum being 0.41 °C per decade for April and the minimum 0.23 °C per decade for May. Except for a few parts of southern Shaanxi and southern Xinjiang in June and August, the temperature increased across the region in all months. The rates of temperature change

in northern Qinghai were relatively high in all months, whereas in Ningxia, Shaanxi and western Xinjiang they were generally low. The overall annual rates of change of precipitation for the period 1959 to 2019 were also positive, with a maximum of 1.8 mm per decade in June and a minimum of 0.12 mm per decade in October.

There has been an obvious spatial displacement of the trends towards warmer and wetter conditions during the study period. The warming trend has tended to shift from bare land regions to grassland regions, while the trend towards increased precipitation has tended to move in the opposite direction. In most parts of northwest China, the trend in the dryness index has been downwards, especially in western Xinjiang and Qinghai. Areas where the dryness index has increased are mainly located in Shaanxi, Ningxia, southern Gansu and northeast Xinjiang. There is a strong spatial correlation between drought and precipitation in northwest China, with the regions of decreasing drought being consistent with the regions of increasing precipitation.

Acknowledgments

This study was supported by National Natural Science Foundation of China (grant number 42071329). The authors acknowledge the National Climate Central, China Meteorological Administration for providing the meteorological data for this study. We acknowledge Dr Christopher C. Hall at University of Technology Sydney, Australia for his writing assistance. We thank the anonymous reviewers for their time and helpful suggestions.

Data availability statement

The data that support the findings of this study are available upon reasonable request from the authors.

ORCID iDs

Shijun Zheng https://orcid.org/0000-0002-8034-5011
Qiaoyun Xie https://orcid.org/0000-0002-1576-6610

References

Allen R G, Pereira L S and Smith M 1998 *Crop Evapotranspiration-Guidelines for Computing Crop Water Requirements-FAO Irrigation and Drainage Paper 56* (Rome: FAO)

Bao Y, Braeuning A, Yafeng S and Fahu C 2004 Evidence for a late Holocene warm and humid climate period and environmental characteristics in the arid zones of northwest China during 2.2 ~ 1.8 kyr B.P *Journal of Geophysical Research: Atmospheres* **109** D02105

Bonan G B, Pollard D and Thompson S L 1992 Effects of boreal forest vegetation on global climate *Nature* **359** 716–8

Burn D H and Elnur M A H 2002 Detection of hydrologic trends and variability *J. Hydrol.* **255** 107–22

Chauhan B S, Mahajan G, Randhawa R K, Singh H and Kang M S 2014 Global warming and its possible impact on agriculture in India *Advances in Agronomy* **123** 65–121

Chen J M 2021 Carbon neutrality: Toward a sustainable future *The Innovation* **2** 100127

Chen S, Shi Y and Guo Y 2010 Temporal and spatial variation of annual mean air temperature in arid and semiarid region in northwest China over a recent 46 year period *Journal of Arid Land* **2** 87–97

Chen Y, Yang Q, Luo Y, Shen Y, Pan X, Li L and Li Z 2012 Ponder on the issues of water resources in the arid region of northwest China *Arid Land Geography* **35** 1–9

Dong B and Dai A 2017 The uncertainties and causes of the recent changes in global evapotranspiration from 1982 to 2010 *Clim. Dyn.* **49** 279–96

Frasier G W, Cox J R and Woolhiser D A 1987 Wet-dry cycle effects on warm-season grass seedling establishment *Journal of Range Management* **40** 2–5

Guo B, Zhang J, Meng X, Xu T and Song Y 2020 Long-term spatio-temporal precipitation variations in China with precipitation surface interpolated by ANUSPLIN *Sci. Rep.* **10** 81

IPCC 2021 *Climate Change 2021: The Physical Science Basis. Contribution of Working Group I to the Sixth Assessment Report of the Intergovernmental Panel on Climate Change* (Cambridge: Cambridge University Press)

Jeppesen E, Beklioğlu M, Özkan K and Akyürek Z 2020 Salinization increase due to climate change will have substantial negative effects on inland waters: a call for multifaceted research at the local and global scale *The Innovation* **1** 100030

Kara B, Atar B and Gul H 2012 Effects of different sowing dates on protein, sugar and dry matter of sweet corn *Research on Crops* **13** 493–7

Li B, Chen Y, Chen Z, Xiong H and Lian L 2016 Why does precipitation in northwest China show a significant increasing trend from 1960 to 2010? *Atmos. Res.* **167** 275–84

Li B, Chen Y, Shi X, Chen Z and Li W 2013 Temperature and precipitation changes in different environments in the arid region of northwest China *Theor. Appl. Climatol.* **112** 589–96

Liao S and Li Z 2003 A methodology of spatialization of observed data based on GIS *Progress in geography* **22** 87–93

Liao S, Li Z and You S 2003 Comparison on methods for rasterization of air temperature data *Resources Science* **25** 83–8

Liu X, Zhang D, Luo Y and Liu C 2013 Spatial and temporal changes in aridity index in northwest China: 1960 to 2010 *Theor. Appl. Climatol.* **112** 307–16

Lu A, Ding Y, Pang H, Yuan L and Yuanqing H 2005 Impact of global warming on water resource in arid area of northwest China *Journal of Mountain Science* **2** 313–8

Meehl G A, Washington W M, Collins W D, Arblaster J M, Hu A, Buja L E, Strand W G and Teng H 2005 How much more global warming and sea level rise? *Science* **307** 1769–72

Mohd Wani J, Sarda V K and Jain S K 2017 Assessment of trends and variability of rainfall and temperature for the district of mandi in Himachal Pradesh, India *Slovak Journal of Civil Engineering* **25** 15–22

Piao S, Ciais P, Huang Y, Shen Z, Peng S, Li J, Zhou L, Liu H, Ma Y and Ding Y 2010 The impacts of climate change on water resources and agriculture in China *Nature* **467** 43–51

Piao S L, Fang J Y, Liu H Y and Zhu B 2005 NDVI-indicated decline in desertification in China in the past two decades *Geophys. Res. Lett.* **32** 347–54

Qian S A, Fu Y and Pan F F 2010 Climate change tendency and grassland vegetation response during the growth season in three-river source region *Science China-Earth Sciences* **53** 1506–12

Ren P, Zhang B, Zhang T, Li X, Chen L and Lu L-P 2014 Trend analysis of meteorological drought change in Northwest China based on standardized precipitation evapotranspiration index *Bulletin of Soil and Water Conservation* **34** 182–7

Sacks W J, Deryng D, Foley J A and Ramankutty N 2010 Crop planting dates: an analysis of global patterns *Global Ecol. Biogeogr.* **19** 607–20

Shi Y, Shen Y and Hu R 2002 Preliminary study on signal, impact and foreground of climatic shift from warm-dry to warm-humid in Northwest China *Journal of Glaciology and Geocryology* **24** 219–26

Shi Y, Shen Y, Kang E, Li D, Ding Y, Zhang G and Hu R 2007 Recent and future climate change in northwest China *Clim. Change* **80** 379–93

Smith C, Nicholls Z R J, Armour K, Collins W, Forster P, Meinshausen M, Palmer M D and Watanabe M 2021 The earth's energy budget, climate feedbacks, and climate sensitivity supplementary material *Climate Change 2021: The Physical Science Basis. Contribution of Working Group I to the Sixth Assessment Report of the Intergovernmental Panel on Climate Change* ed V Masson-Delmotte *et al* (Cambridge: Cambridge University Press)

Tian H, Xu X, Lu C, Liu M, Ren W, Chen G, Melillo J and Liu J 2011 Net exchanges of CO_2, CH_4, and N_2O between China's terrestrial ecosystems and the atmosphere and their contributions to global climate warming *J. Geophys. Res.* **116**

Wang A, Miao Y and Chen Y 2020 Interdecadal variation of land water budget in Northwest China from 1961 to 2016 *Transactions of Atmospheric Sciences* **43** 953–66

Wang H, Chen Y and Chen Z 2013 Spatial distribution and temporal trends of mean precipitation and extremes in the arid region, northwest of China, during 1960–2010 *J Hydrological Processes* **27** 1807–18

Wang P, He J, Zheng Y and Zhang Q 2007 Aridity-wetness characteristics over Northwest China in recent 44 years *Journal of Applied Meteorological Science* **18** 769–75

Yan H, Zhou M, Xu Z, Wang Q, Liu J, Zhou Y, Wang N and Ding D 2020 Effect of sowing date on winter wheat yield and yield composition in Jiangsu Province *Agricultural Research in the Arid Areas* **38** 293–302

Yang J, Jiang Z, Liu X and Yue P 2012 Influence research on spring vegetation of Eurasia to summer drought-wetness over the northwest China *Arid Land Geography* **35** 10–22

Zhai P M, Zhang X B, Wan H and Pan X H 2005 Trends in total precipitation and frequency of daily precipitation extremes over China *J. Clim.* **18** 1096–108

Zhang H L, Zhang Q, Yue P, Zhang L, Liu Q, Qiao S B and Yan P C 2016 Aridity over a semiarid zone in northern China and responses to the East Asian summer monsoon *Journal of Geophysical Research-Atmospheres* **121** 13901–18

Zhang Q, Yang J H, Wang W, Ma P L, Lu G Y, Liu X Y, Yu H P and Fang F 2021 Climatic warming and humidification in the arid region of Northwest China: multi-scale characteristics and impacts on ecological vegetation *Journal of Meteorological Research* **35** 113–27

Zhao L, Dai A and Dong B 2018 Changes in global vegetation activity and its driving factors during 1982–2013 *Agric. For. Meteorol.* **249** 198–209